Journal of Marine Science and Technology
DOI: 10.6119/JMST-012-1005-1

A HEAT ISLAND OBSERVATION VIA MODIS AND CONCURRENT HELICOPTER-BORNE IR IMAGER

Tsung-Hua Kuo[1], Gin-Rong Liu[1], Tang-Huang Lin[1],
Chia-Wen Lan[2], and Chi-Ping Huang[2]

Key words: heat island, MODIS, NDVI.

ABSTRACT

In this study, observations and aerial surveys were conducted in delineating the heat island patterns. Concurrent datasets from the satellite-borne MODIS sensor and helicopter-borne th ermal IR imager were employed. The sampling data in this experiment covered an area exceeding 100 km^2 in Taiwan's western plain. A more than 10°C temperature difference between different sampling points could be observed in this area. The relationship between the surface temperature and vegetation index values was also showed. Results showed that the surface canopy and the air humidity together played an important role in the surface temperature increase.

I. INTRODUCTION

Currently, one of the most well known climate impact factors is the heat island effect caused by urbanization [12, 14]. In the past decades, changes in the landcover or heat sources by human activities have significantly altered the surface (especially for urban areas), and has become one of the key contributors to global change. The impact from global changes is one of the most important issues concerning not only scientists but the general public as well. In fact, a growing amount of evidence obtained from ground truth and satellite observations shows that the influence from human activities can seriously affect the Earth's climate and biosphere [2, 5, 11]. Understanding how man-made heating mechanisms affect the environment can provide us with insights in knowing how to devise appropriate solutions. Therefore, research studies covering this topic, especially with remote sensing data are strongly recommended.

As an example, the population density of Taiwan is one of the highest in the world. More than 23 million people live on the island, which covers an area of only about 36,000 km^2. However, more than two thirds of the land surf ace is mountainous terrain, rendering most of the population to be concentrated on the western plains. As Taiwan's industrialization and population clustering have grown tremendously over the past decades, the urbanization has inevitably altered the landuse/landcover pattern types. The growth in the population, cars, air conditioners, industrial parks and so forth have resulted in the land surface to emit more heat to the environment [8, 15]. The heating process is seen to be closely related to the degree of urbanization [3, 17]. Referred as the heat island effect, the phenomena have been documented for almost one and half centuries [4]. However, only recently has this become an important research issue, as it is considered a serious factor in the global warming debate [7, 10]. The heating changes the environmental heat distribution, resulting in higher air and land surface temperatures in the urban areas when compared to the nearby rural areas. By average, the temperature can increase by more than 4°C [13]. The higher temperature and concentration of artificial concrete surfaces and asphalt roads can strongly influence the evapotranspiration process between the air-land interactions, thereby creating a huge impact on the environment.

In light of this issue, a heat island observation experiment of Taiwan was conducted by this study to better understand how urbanization induces the heat island effect. MODIS satellite observations coupling with ground truth data collected from weather stations and helicopter-borne thermal IR Imager sensors were utilized. A preliminary heat island pattern was constructed by this study. The relationship between the surface canopy vegetation index values and heat island formation will be discussed in the following sections.

II. DATA

The data used in this study are shown as follows: Helicopter-borne thermal IR imager, MODIS, weather station data, and automatic weather recorders [16]. The first two platforms provide the thermal IR images for the surface temperature retrieval, while the surface temperature, humidity, and wind speeds are

Paper submitted 05/13/11; revised 05/18/12; accepted 10/05/12. Author for correspondence: Gin-Rong Liu (e-mail: GRLiu@csrsr.ncu.edu.tw).
[1]Center for Space and Remote Sensing Research, National Central University, Chung-Li, Taiwan, R.O.C.
[2]Institute of Atmospheric Physics, National Central University, Chung-Li, Taiwan, R.O.C.

provided by the weather stations.

The thermal IR Imager (ThermoVision A40M) was manufactured by the FLIR Systems Incorporation. The imager is a very compact infrared imaging and temperature measurement camera. It provides high resolution IR images, which is dependent on the flying height. Each thermal image is built from 76,800 individual picture elements that are sampled in real time. The A40M is capable of seeing temperature variations as small as 0.08°C. It has a solid state, uncooled microbolometer detector covering 7.5 to 13μm, and provides -40°C to +70°C storage temperature range. In this experiment, the camera was mounted under a Bell helicopter [1].

In order to provide a large coverage area, the MODIS (or Moderate Resolution Imaging Spectroradiometer) images were used. Carried onboard the Terra (EOS AM) and Aqua (EOS PM) satellites, it acquires data in 36 spectral bands in the visible, near IR and thermal IR regions. Currently, the MODIS satellite plays a vital role in offering integrated remotely sensed data for the monitoring and analysis of our environment [6].

To verify the satellite-borne and helicopter-born temperature observations, this study also gathered temperature and wind speed data from ground weather stations, where they were either operated by Taiwan's Central Weather Bureau (CWB) or agricultural institutions. Furthermore, in addition to these stations, data from several automatic weather recorders located in Chia-Yi City and its surrounding suburban areas were also used to help acquire an even more detailed map of the surface weather.

III. HELICOPTER OBSERVING EXPERIMENT

The western plains of Taiwan (primarily Chia-Yi City and County) were chosen as the study's investigation area, as it contained various surface canopies, cities, villages, mountains, farms, waterbodies…etc. This could provide an opportunity in comparing the various influences from different landcovers.

The main observations were conducted on Dec 27, 2006. Figure 1 shows the helicopter routes over the test area recorded by the GPS instrument. In order to retrieve as much data as possible, we conducted a cross flying path that covered larger areas and more landcover types. Most of the IR images were taken at an altitude between 600 to 800 meters (most cases were at an altitude of 600 meters) for the aerial observations. This slowed down the flying speed, as the helicopter needed to obtain a good focus and reduce the amount of blurry images taken at every location.

In this analysis, the infrared images acquired by satellites and helicopter-borne IR imager were converted into brightness temperatures in depicting the surface temperature by the inverse of the Planck function,

$$Ti(Ri) = C2\nu_j / \ln(1 + C1\nu_j^3 / Ri) \qquad (1)$$

where T is the brightness temperature (K) for the radiance value R, $C1$=1.1910659×10^{-5} mWm^{-2}sr^{-1}cm^4 and $C2$= 1.438833 cmK, ν is their central wave number for the thermal IR channel, i and j are the observed target and thermal IR channel, respectively. Theoretically, a water vapor correction can be conducted to acquire a more accurate temperature estimation if two infrared channels are employed simultaneously [9, 18]. Such an atmospheric correction technique is already considered very mature for the NOAA/AVHRR channels. However, one infrared channel is considered sufficient for general resource surveillances and skin temperature pattern retrieval.

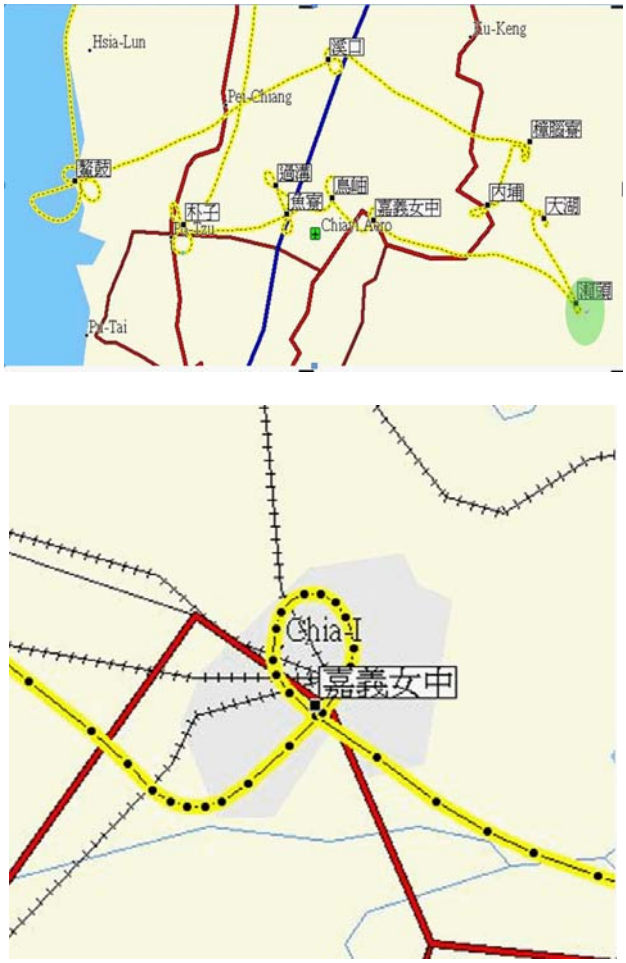

Fig. 1. The upper panel shows the helicopter flight path of the heat island experiment. The locations written in Chinese reveal the sampling points of this study. The path begins from the far left, and moves in a clockwise direction to other sites. The lower panel shows a more detailed description of a particular location.

Meanwhile, the MODIS data were employed to access the vegetation canopy in comparing the relationship with the surface skin temperature. The normalized difference vegetation index or NDVI graphs were employed and derived from the MODIS bands,

$$\text{NDVI} = (\text{near IR} - \text{visible}) / (\text{near IR} + \text{visible}) \qquad (2)$$

Generally, the near IR represents the frequencies at 0.72~1.1μm, and the visible frequency encompasses the

0.58~0.68μm wavelengths. In terms of the MODIS data, we used channel 1 (0.62-0.67μm) and channel 2 (0.84-0.87μm). The NDVI values, which range from 0 to 1, could be used as an indicator of the vegetation's greenness (green biomass) or density. In other words, larger values indicate darker/forest vegetation canopy and smaller values depict less dense canopy, bare soil or even city/building areas.

IV. RESULTS AND DISCUSSIONS

Figure 2 shows some of the images acquired by the helicopter-borne IR Imager. During the observation, a portable GPS was used to record the (longitude, latitude, elevation) coordinates with time. Based upon the subsequent data checks and comparisons with the Google map satellite images, the GPS records were precise enough for our analysis. The temperature variations caused by different targets (emissivity) are clearly shown.

In the experiment, the IR imager images were taken at an altitude of 600 to 800 meters. The acquired images generally covered a limited area only. The small coverage area made the location registration difficult to conduct. However, with the aid of high resolution satellite images, most of the surface points could be located for analysis. Through the employment of the ThermaCAM Research 2.8 software package provided by the FLIR System, the surface temperature could be converted from the acquired images. However, the influence from the atmospheric effects was not taken into account. An atmospheric correction procedure should be considered for future analysis if a rigid accurate comparison is required. Since several of the different landcover types could generally appear during a FOV scanning procedure, the statistical medium values gathered from this analysis could be considered as the nominal temperature of the single scanning observation.

The IR images acquired by the helicopter could be converted into surface temperature maps. The maps clearly showed that the surface temperature was strongly dependent with the corresponding landcover types. Generally, artificial surfaces, such as houses, buildings, roads, cars…etc, had higher temperatures, while the lower temperature essentially appeared in dense vegetation canopy areas. However, the high resolution images taken by the IR imager only covered a small area per scene, due to its low flying altitude and small field-of-view (FOV).

In order to obtain a comprehensive heat distribution of the selected area, the MODIS data was utilized. From the thermal bands in the MODIS platform, a large land surface temperature (LST) map could be obtained (Figure 3). The temperature map clearly revealed that the left part of the test area obviously had a higher temperature distribution than the right portion, and the temperature values decreased as the vegetation canopy increased. The temperature values varied from 18 to 36°C. The highest values occurred in the eastern parts of Pu-Tzu, while the lowest values were seen in the eastern part (Ta-Hu and Chang-Nao-Liao) of the observation area. This probably was caused by the low cloud layers and higher landscape. Once again, we used the MODIS red and near IR bands to calculate the NDVI map, which was a simple but efficient indicator for finding the dense or isolated vegetation areas (Figure 4). The contrast between Figures 3 and 4 demonstrates that the main surface heating was caused from deforestation, reduction of vegetation areas, and increase of artificial surfaces.

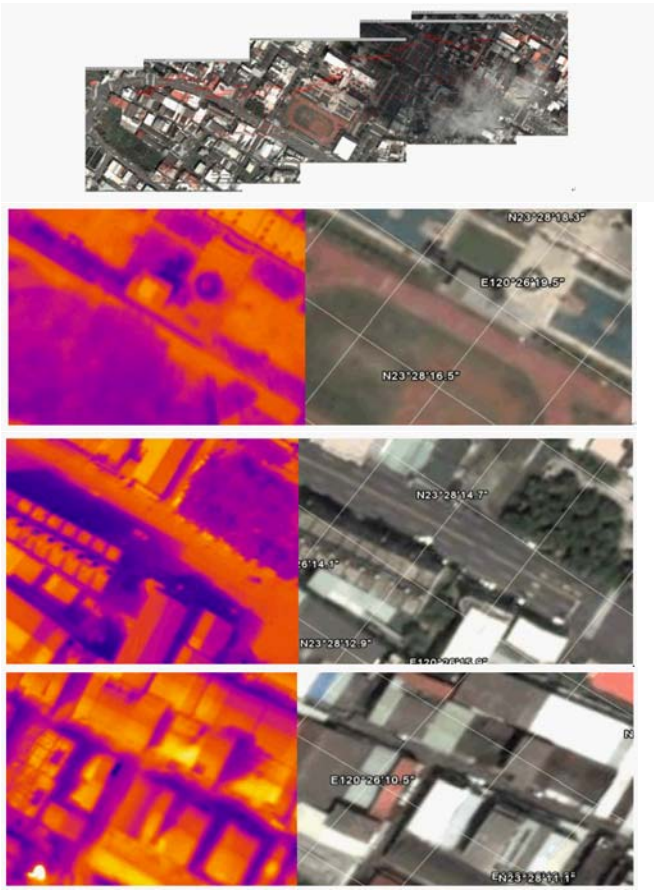

Fig. 2. Examples of images acquired by the helicopter-borne IR Imager (red-blue images). The right panels correspond to the high resolution satellite images (true color images) from the Google map.

After obtaining the surface temperature, the relationships between the MODIS LST, IR Imager LST and station measured temperatures for the sampling locations can be seen in Figure 5. Some measurements were discarded due to poor data quality, which was probably induced by instrumental errors and inaccurate GPS positioning. The temperatures at some stations were obviously lower than the other stations, likely caused by more haze conditions and a higher landscape. Moreover, the higher surface temperature appeared in the downtown CYGS station.

Compared to the MODIS measurements, the helicopter-IR Imager measurement had the maximum correlation with the station temperature. This means that comparisons between different remotely sensed data to the ground truths need to consider the spatial resolution scale carefully. The relationship of the surface temperature observed by the IR Imager with the

NDVI values and near surface relative humidity was also investigated (Figures 6 and 7). It is reasonable that the results showed a high correlation between the temperature and NDVI. Needless to say, the (decreasing) change of the vegetation canopy plays a very important role in the growth of heat islands. In addition, the water vapor in the air also owned an evident (but not as high as the previous one) negative correlation with the surface temperature. However, due to the mutual interaction between temperature, vegetation, and water vapor (humidity), more studies are needed to understand the individual and integrated contributions by these variables.

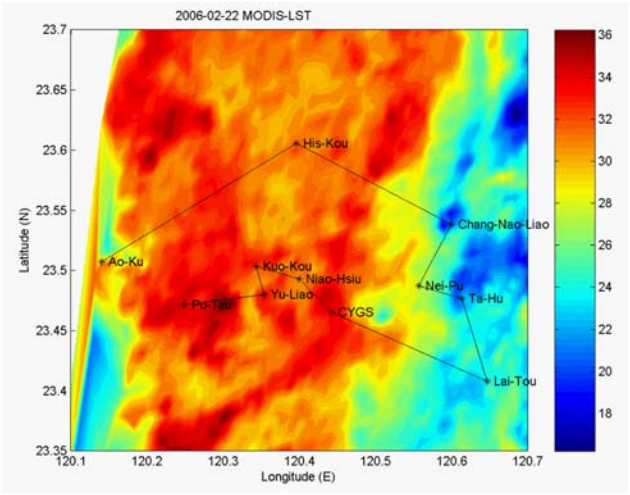

Fig. 3. The land surface temperature map derived by concurrent observations from MODIS thermal IR bands.

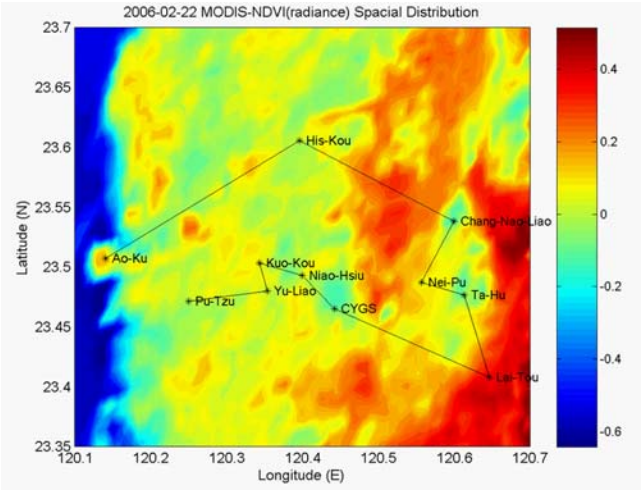

Fig. 4. Same as Figure 3, but an NDVI map.

Overall, the three temperature datasets gathered from the IR imager, MODIS and ground stations showed a good match. The consistency between MODIS and helicopter Imager-retrieved temperature was still very strong. However, the same relationship was not exhibited for the ground-measured temperature, thereby causing errors in the GPS positioning accuracy. This may be partly attributed to influences from the may be partly attributed to influences from the atmosphere. However, the inconsistency requires further analysis before it can be more aptly addressed. It is shown that the RH has a nontrivial relationship with the temperature.

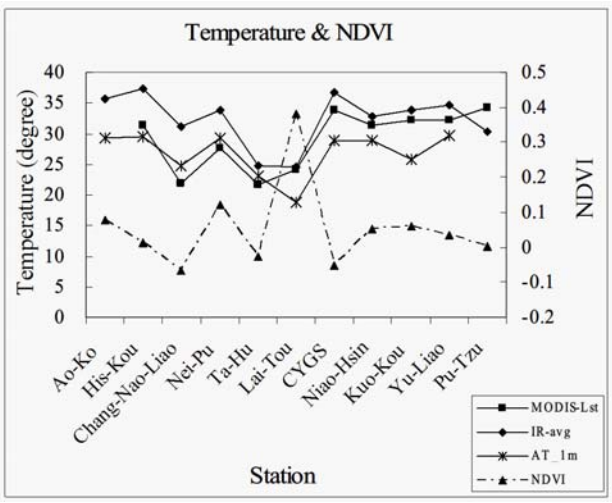

Fig. 5. The relationships between MODIS LST, IR Imager LST and station measured temperatures for the sampling locations.

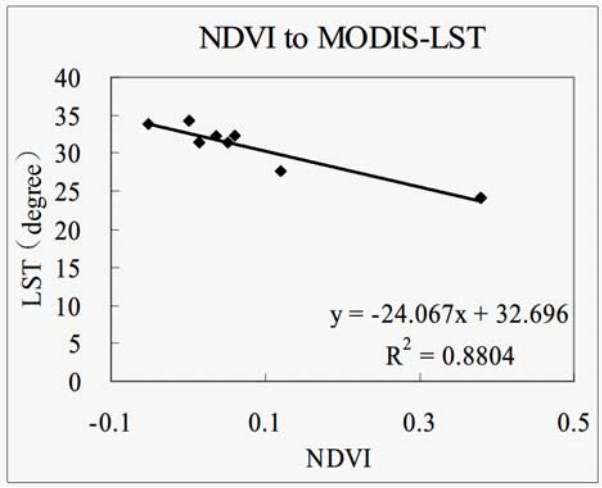

Fig. 6. Relationship between the land surface temperatures with the NDVI index.

V. CONCLUSION

The heat island effect has been discussed for more than a century. However, the issue has only become an important research topic in the past few decades, due to the rapid urbanization of many cities and areas. The effect is worsening, as many of these cities are evolving into so-called “megacities”. In addition, the mutual interaction between global warming and the heat island effect may cause the latter to deteriorate further. Therefore, further research and observations regarding this issue are necessary. One of the main tasks of this study is to establish a concurrent helicopter-borne observation procedure,

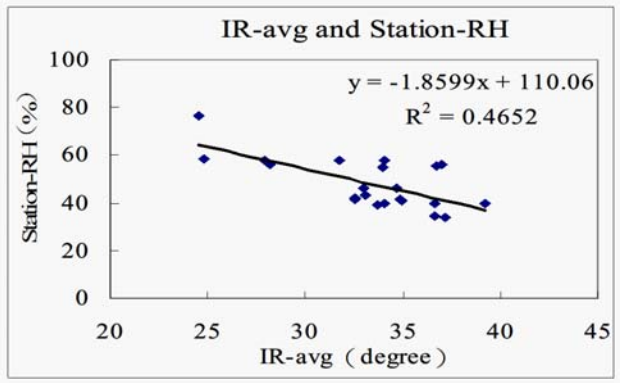

Fig. 7. Relationship between the surface relative humidity with the land surface temperature.

which can serve as a supplement to satellite observations. The data gathering via an airborne platform delivers higher resolution images, providing more in-depth details of a specific area. The information can be used together with satellite observations. Assimilation of the two types of data can be very useful to landuse/landcover survey, precision agriculture, disaster investigation, disaster relief and so forth. This is demonstrated by this study, where the thermal IR Imager, ThermoVision A40M, was employed to test and establish a mobile airborne observation procedure. The flying routes, sampling points, and helicopter flying altitude were all tested in establishing a standard operation procedure for future missions. The flying observation experiment showed that the A40M imager carried by a helicopter could retrieve high resolution images in both the visible and thermal channels. However, the concurrent observations also showed that improvements can still be made on the positioning technique. The inaccurate positioning sometimes rendered the images being unable to match with the satellite images or maps, thereby limiting relevant precise analysis applications.

From both the helicopter and satellite observations, the heat island pattern is obvious in the western Taiwan Plains. A more than 10°C temperature difference can be observed between the different landcover and vegetation canopy. The result clearly demonstrates the close negative relationship between the vegetation influences and surface temperature. Meanwhile, the humidity has a weaker relationship with the temperature. To further understand the thermal radiation interaction among these parameters during a heat island effect, employment of the radiation transfer models are recommended. If possible, an accurate model taking into account the influence of aerosols, artificial surfaces, and surface waterforms is recommended to compute the heat flux, which will enable a better understanding of the sources and sinks of the heat island heating process.

Acknowledgments. The authors thank Prof. Shih-Jen Huang from Department of Marine Environmental Informatics, National Taiwan Ocean University for his great help in the airborne observation experiment. This research was supported by the National Science Council Grant NSC 100-2621-M-008-008.

REFERENCES

1. FLIR Stems, *Thermovision A40M Operator's Manual*, FLIR Systems, Publ. No. 1557813, pp. 222 (2004).
2. Gallo, K. and Owen, T. W., "Satellite-based adjustments for the urban heat island temperature bias," *Journal of Applied Meteorology*, Vol.8, No.6, pp. 806-813 (1999).
3. Henry, J. A., Dicks, S. E., Wetterqvist, O. F., and Roguski, S. J., "Comparison of satellite, ground-based, and modeling techniques for analyzing the urban heat island," *Photogrammetric Engineering and Remote Sensing*, Vol.55, No.1, pp. 69-76 (1989).
4. Howard, L., *The climate of London*, Vols. I-III, Harvey and Dorton (1833).
5. Hung, T., Uchihama, D., Ochi, S. and Yasuoka, Y., "Assessment with satellite data of the urban heat island effects in Asian mega cities," *International Journal of Applied Earth Observation and Geoinformation*, Vol.8, No.1, pp. 34-48 (2006).
6. Jin, M. E., Dickinson, R., and Zhang, D. L., "The footprint of urban areas on global climate as characterized by MODIS," *Journal of Climate*, Vol.18, No.10, pp. 1551-1565 (2005).
7. Kato, S. and Y. Yamaguchi, "Analysis of urban heat-island effect using ASTER and ETM+ data: separation of anthropogenic heat discharge and natural heat radiation from sensible heat flux," *Remote Sensing of Environment*, Vol.99, No.1-2, pp. 44-54 (2005).
8. Liu, H. and Weng, Q., "Seasonal variations in the relationship between landscape pattern and land surface temperature in Indianapolis," *U.S.A. Environmental Monitoring and Assessment*, Vol.144, No.1, pp. 199-219 (2008).
9. Price, J. C., "Land surface temperature measurements from the split window channels of the NOAA 7 Advanced Very High Resolution Radiometer," *Journal of Geophysical Research*, Vol.89, No.D5, pp. 7231-7237 (1984).
10. Rosenzweig, C., Solecki W. D., Parshall, L., Chopping, M., Pope, G., and Goldberg, R., "Characterizing the urban heat island in current and future climates in New Jersey," *Environmental Hazards*, Vol.6, pp. 51-63 (2005).
11. Rajasekar, U., and Weng, Q., "Spatio-temporal modelling and analysis of urban heat islands by using Lansat TM and ETM+ imagery," *International Journal of Remote Sensing*, Vol.30, No.13, pp. 3531-3548 (2009).
12. Sarrat, C., Lemonsu, A., Masson, V., and Guedalia, D., "Impact of urban heat island on regional atmospheric pollution," *Atmospheric Environment*, Vol.40, No.10, pp. 1743–1758 (2006).
13. Streutker, D. R., "Satellite-measured growth of the urban heat island of Houston, Texas," *Remote Sensing Environment*, Vol.85, No.3, pp. 282-289 (2003).
14. Tomlinson, C. J., Chapman, L., Thornes, J. E., and Baker, C. J., "Derivation of Birmingham's summer surface urban heat island from MODIS satellite images," *International Journal of Climatology*, Vol.32, No.2, pp. 214-224 (2010).
15. Voogt, J. A. and Oke, T. R., "Effects of urban surface geometry on remotely sensed surface temperature," *International Journal of Remote Sensing*, Vol.19, No.5, pp. 895-920 (1998).
16. Wan, Z., "New refinements and validation of the MODIS land-surface temperature/emissivity products," *Remote Sensing of Environment*, Vol.112, No.1, pp. 59-74 (2008).
17. Wang, W. C., Zeng, Z., and Karl, T. R., "Urban heat islands in China," *Geophysical Research Letters*, Vol.17, No.12, pp. 2377-2380 (1990).
18. Weng, Q., "Thermal infrared remote sensing for urban climate and environmental studies: Methods, applications, and trends," *Journal of Photogrammetry and Remote Sensing*, Vol.64, No.4, pp. 335-344 (2009).